Fate of silver nanoparticles in constructed wetlands – a microcosm study

Hannele Auvinen[a,b*], Ralf Kaegi[c], Diederik P.L. Rousseau[b], and Gijs Du Laing[a]

a Laboratory of Analytical Chemistry and Applied Ecochemistry, Faculty of Bioscience Engineering, Ghent University, Coupure Links 653, 9000 Gent, Belgium.

b Laboratory of Industrial Water and Ecotechnology, Faculty of Bioscience Engineering, Ghent University Campus Kortrijk, Graaf Karel de Goedelaan 5, 8500 Kortrijk, Belgium

c Eawag, Swiss Federal Institute of Aquatic Science and Technology, Überlandstrasse 133, 8600 Dübendorf, Switzerland

* Corresponding author:

E-mail address: Hannele.Auvinen@UGent.be

Tel:+32 56 24 12 11

Fax: +32 56 24 12 24

Abstract

Nano-enabled materials are produced at growing volumes which increases the likelihood of nanoparticles being released into the environment. Constructed wetlands (CWs) are likely to receive wastewater containing nanoparticles leaching from products during usage. Therefore, we investigate the retention of silver nanoparticles (Ag-NPs) in microcosms simulating CWs treating domestic wastewater. The effects of aeration and organic matter content on the Ag-NP removal efficiencies are studied in particular. CWs remove most of the Ag (80 % - 90 %) and the largest fraction of Ag is found in/on the biofilm. Detailed electron microscopy analyses suggest that Ag-NPs are transformed into Ag_2S in all microcosm experiments. The good correlation between total suspended solids (TSS) and the Ag concentration measured in the effluent indicates that Ag-NPs are bound to the solids in the effluent. Aeration of the

microcosms does not affect the release of Ag-NPs from the systems but increasing organic matter leads to increased amounts of Ag passing the CWs, correlating with the increased release of TSS from the CWs. These results suggest that Ag-NPs are retained with the (suspended) solids in CWs and that the removal efficiency of TSS is an important factor determining the discharge of Ag-NPs from CWs.

Key words

Constructed wetland, silver nanoparticle, nanomaterial, ICP-MS, STEM-EDX, sulfidation, wastewater

1. Introduction

Silver nanoparticles (Ag-NPs) are used in common household products, such as textiles, biocidal sprays, food packaging material and toys, because of their antimicrobial properties (The Project of Emerging Nanotechnologies: Consumer Product Inventory, 2016). During washing, Ag-NPs can be released from textiles (Benn & Westerhoff, 2008; Mitrano et al., 2014) and will thus be transported to the wastewater treatment plant through the municipal sewer system. Even though the concentration of Ag-NPs in the raw wastewater is currently low (Li et al., 2013), the predicted increase in their production and use may lead to elevated amounts of Ag-NPs released into the wastewater in the future (Peralta-Videa et al., 2011). The specific use of Ag-NPs in household products in combination with the toxicity of Ag (Doiron et al., 2012; Ratte, 1999) and the resulting environmental risk (Colvin, 2004), have led to several scientific publications studying the removal of Ag-NPs from wastewater streams (Kaegi et al., 2013; Lombi et al., 2013).

These studies revealed that sulfidation of Ag-NPs and attachment of Ag-NPs to sludge biomass are the most important processes mitigating the toxicity of Ag-NPs (Reinsch et al.,

2012) and removing them from the wastewater stream through sedimentation in a secondary clarifier. According to Kaegi et al. (2011), sulfidation of Ag-NPs is a fast process and at current Ag concentrations measured in wastewater, is neither limited by the sulfide availability in the wastewater nor by the hydraulic retention time in wastewater systems. Due to the efficient removal of Ag-NPs during the wastewater treatment (sulfidized) Ag-NPs will be accumulated in the sewage sludge. Kim et al. (2010) identified individual nanosized silver sulfide particles in the sludge of a full-scale wastewater treatment plant. In a microcosm study simulating emergent freshwater wetland, spiked Ag-NPs quickly settled to the bottom and transformed into Ag_2S (Lowry et al., 2012a), further demonstrating the importance of the sulfidation of Ag-NPs.

The removal of engineered nanoparticles (NPs) in constructed wetlands (CWs) has received little attention to date. CWs are often applied for domestic wastewater treatment, usually in remote areas and small communities, and can also be used to treat landfill leachate among others types of wastewater (Kadlec & Wallace, 2009). Different compositions of the influent water, different designs, operation principles and varying ages of the CWs affect the conditions within the CWs, for example, oxygen content, redox conditions, retention time, and accumulation of organic matter within the CWs. Aeration of CWs enhances their treatment efficiency (Fan et al., 2013; Nivala et al., 2007; Zhang et al., 2010), but aeration may result in the release of Ag^+ due to the oxidative dissolution of Ag-NPs (Liu et al., 2011). Ag^+ may be of even greater environmental concern than Ag in its particulate form (Behra et al., 2013). Furthermore, the conditions within CWs can change dynamically over the typical lifetime of CWs (20 – 30 years) owing to changes on a time scale of minutes (e.g. accepting stormwater overflows) to years (e.g. clogging, vegetation development). Physicochemical conditions of the surrounding media influence the transformations of NPs, and thus define the persistence, reactivity, bioavailability and toxicity of (transformed) NPs in the environment

(Lowry et al., 2012b). To assess the risk associated with an increasing use of (Ag)-NPs in consumer products and to better understand the environmental distribution of (Ag-)NPs, it is therefore of interest to study the removal of (Ag-) NPs in CWs.

Therefore, we investigated the retention of Ag-NPs in microcosms simulating CWs treating domestic wastewater and studied the distribution and transformation of Ag-NPs (citrate-coated) within the CW microcosms. Although only one type of Ag-NP was studied, earlier research indicated that coating (citrate or PVP) does not affect the fate of Ag-NPs during wastewater treatment (Kaegi et al., 2013). We derived the removal efficiency of the Ag-NPs by comparing the Ag concentration measured in samples collected from the influent and from the effluent of the CWs. Ag concentrations of the digested biofilm and plant material were used to establish the distribution of Ag within the microcosms and the transformation (sulfidation) of the Ag-NPs in the biofilm was evaluated by detailed electron microscopy analyses. By aerating and adding organic matter (OM) to the microcosms we assessed whether these factors influence the amount of Ag discharged from the microcosms.

2 Materials and methods

2.1 Experimental design

Microcosms simulating sub-surface flow CWs were monitored during this experiment. The experiment lasted for 25 weeks including an initial adaptation period during which the plants were allowed to grow and biofilm to develop before the Ag-NP dosing was initiated. The microcosms were sampled once a week for 18 weeks. To investigate the effect of aeration and OM on the performance of the CWs, different microcosms were set up as shown in Table 1. Aeration is sometimes applied in CWs to stimulate the removal of organic carbon (e.g. Fan et al., 2013), but could also foster the oxidation of Ag-NPs which may affect their fate in the

95 microcosms. During the lifetime of CWs, there is build-up of OM and reed leaves were added
96 to simulate the accumulation of OM in an aging CW.

97 ***Table 1 – Setup of the different treatments. The microcosms were constructed in triplicate for each treatment.***

Microcosm	Aeration applied	OM added	Ag-NP added
Air	X	-	X
OM	-	X	X
Positive control	-	-	X
Negative control	-	-	-

98

99 The microcosms were built in polypropylene containers by filling them with 2 L of washed
100 gravel (∅ 6/8 mm; porosity 36.5 % ± 1.3 %; Kranendonk NV, The Netherlands). A similar
101 setup has been used earlier to assess the effects of ENMs on the microbial community in CW
102 microcosms (Button et al., 2016). A schematic illustration of the setup can be found in Button
103 et al. (2016). The chemical composition and the cation exchange capacity and pH of the
104 gravel used have been reported earlier (Auvinen et al., 2016). The depth of the gravel layer
105 was approximately 15 cm. The microcosms were planted with common reed (*Phragmites*
106 *australis),* obtained from a local garden center. Little amounts of potting soil was still present
107 between the fine roots upon planting. The setups were fitted with a 32-mm-diameter
108 perforated central sampling tube and a small outlet spout made of silicone tubing with a
109 plastic stopper for draining. The aeration was provided in the AIR microcosms with an
110 aquarium air stone and pump (Hozelock 320). The reed leaves added in the OM microcosms
111 were placed in a rain water tank for one month before the beginning of the experiment where
112 the leaves partially degraded. Then, the leaves were chopped in small pieces and 100 g was
113 mixed thoroughly with the gravel.

114 In total, the influent water of the CWs was spiked 18 times with Ag-NPs (50 μg
115 Ag/week/microcosm). The concentration occurring in the microcosms (100 µg/L) was higher

than expected to occur in real domestic wastewater (Blaser et al., 2008) to be able to detect residual Ag via microscopy and measure it in plant material where concentrations were predicted to remain low. Synthetic domestic wastewater (OECD 2001) was used as influent (490 mL per microcosm). The Ag-NPs were added in the influent to guarantee their even distribution of in the microcosm. The spiking of the influent was done individually per microcosm and the synthetic wastewater was added to the microcosm immediately after spiking the wastewater with Ag-NPs to minimize the holding time and possible subsequent transformations of Ag-NPs. In the study of Button et al. (2016) where same synthetic wastewater and Ag-NPs were used, no sulfidation nor chlorination was observed directly after adding the Ag-NPs to the wastewater solution.

The microcosms were operated in batch mode with weekly draining of the effluent equating to a hydraulic retention time (HRT) of 7 days. The microcosms were drained top-down via the outlet spout so that the water was completely replaced by freshly prepared influent. The evaporating water was replaced twice a week with tap water. The effect of the replenished water on the salinity of the water inside the microcosms was expected to be insignificant due to the low volume added in the system (~100 mL/week/microcosm).

2.2 Nanoparticle suspensions

Citrate-coated Ag-NPs were obtained from PlasmaChem GmbH (Berlin, Germany) as a colloidal suspension (pH 6 – 8). The suspension was stored in the dark at 4 – 8 °C. The concentration of the stock dispersion was measured prior to use by inductively coupled plasma-mass spectrometry (ICP-MS) as described later in 2.3.2. The dispersion was digested prior to analysis as described later in 2.3.1 for influent and effluent samples. The Z-average hydrodynamic diameter of the particles in the stock solution was determined by using a Photon Correlation Spectrometer (PCS; 100M Malvern Instruments Ltd). All measurements were performed in triplicate at 25 °C using a helium-neon laser (633 nm) and a scattering

141 angle of 150°. The average particle size was determined based on intensity and number. The
142 particles in the stock suspension were additionally investigated by a scanning transmission
143 electron microscope (STEM) and the particle size distribution was extracted from STEM
144 images using the ParticleSizer software (Wagner, 2016).

145 **2.3 Total silver analysis**

146 2.3.1 *Digestion of the samples*

147 Influent and effluent water samples were digested in the microwave oven (Mars 5 and 6) after
148 adding 4 mL of concentrated HNO_3 and 1 mL of H_2O_2 to 10 mL of sample. The digestion
149 program consisted of the following steps: 10 min at 55 °C; 10 min at 75 °C; 40 min at 100 °C.
150 The performance of the digestion method was investigated as a preliminary study prior to
151 another research project studying the fate of Ag-NPs in natural water samples previously
152 conducted in our lab (Van Koetsem et al., 2015, 2016).

153 At the end of the experiment, total Ag content in the different compartments of the
154 microcosms was also determined. The gravel was mixed carefully after removing the plants
155 and sub-samples of 100 g were treated with 100 mL of potassium-free phosphate buffer (10
156 mM Na_2HPO_4 , 8.5 g/L NaCl, pH 7.4) to detach the biofilm and the organic matter from the
157 gravel (Button et al., 2016). The sample was shaken (orbital shaker) in the buffer solution for
158 2 h at moderate speed (200 rpm), after which the buffer was directly decanted. A sub-sample
159 of 10 mL was digested following the protocol described above and the Ag concentration was
160 measured to assess the fraction of Ag associated with the biofilm and the organic matter. To
161 the remaining gravel sample 20 mL of 5 % HNO_3 was added to allow the determination of Ag
162 firmly attached to the gravel. After shaking the sample for 1 h at moderate speed (200 rpm),
163 the acidic solution was directly decanted and 10 mL of sample was digested as described
164 above. These sequential extractions were conducted in duplicate for each microcosm.

To determine the amount of Ag attached to the biofilm on the microcosm walls, 100 mL of 5 % HNO_3 and 5 mL H_2O_2 were added to the empty container after the experiment and shaken vigorously. 10 mL of sample were digested and analyzed for total Ag as described above.

The plant samples were divided in two parts: aboveground tissue (i.e. stems and leaves) and belowground tissue. Due to the very fine structure of the roots, these samples may still have contained small amounts of potting soil. Both types of plant samples were dried in an oven overnight (40°C), cut into pieces and ground to a fine powder with mortar and pestle. A sub-sample of 1 g of plant material was digested as described in Du Laing et al. (2003). Minor amounts of particulate matter were still observed in the digest. This material was left to settle, and only the supernatant was used for the analysis of total Ag.

2.3.2 Analysis of Ag

Digested samples (<15 mL) were first diluted to 25 mL with Milli-Q water and then diluted (1:10) with an acidified (1 % HNO_3) internal standard (10 µg Ga/L and 10 µg Rh/L) solution. Thereafter, the total silver concentration was measured using ICP-MS (PerkinElmer Sciex Elan DRC-e). The instrumental parameters and the calibration ranges are given in the supplementary information section. External calibration standards were used for ICP-MS analyses, and recalibrations were performed every 20 samples. Blank samples and reference standards were included at the beginning and the end of each intra-analysis batch of 20 samples for quality control purposes. The detection limit varied during the experiment between 0.02 and 0.12 µg Ag/L. The detection limit was defined as the sum of the average Ag concentration measured in blank samples and 3 times standard deviation of these samples.

2.4 Total organic carbon, total suspended solids, dissolved oxygen and pH

Thirteen weeks after the beginning of the Ag-NP spiking, total organic carbon (TOC) and total suspended solids (TSS) were determined on effluent samples weekly for five weeks.

189 TOC was measured in non-filtered samples using a TOC-analyzer (TOC-V_{CPN}, Shimadzu).
190 The detection limit of these measurements varied between 1.2 and 3.9 mg/L. The detection
191 limit was defined as the sum of the average TOC concentration measured in blank samples
192 and 3 times standard deviation of these samples. TSS was determined gravimetrically after
193 filtering 100 mL of effluent through a paper filter (Macherey Nagel 640m). The total Ag
194 concentration in the filtrate was determined twice (analysis as described earlier in 2.3.1 and
195 2.3.2).

196 The dissolved oxygen (DO) content in the microcosms was measured twice during the
197 experiment (week 4 and 7) by using a portable DO meter (HI9142, Hanna Instruments). The
198 DO was measured *in situ* 3-4 days after spiking of Ag-NPs by using the perforated sampling
199 tube inside the microcosm. The pH was measured twice during the experiment (week 4 and 7)
200 from the influent and drained effluents by using a bench-top pH meter (520A, Orion Research
201 Inc.).

202 **2.5 STEM-EDX**

203 Samples from the stock suspension and from the biofilm extracts were analyzed using a
204 scanning transmission electron microscope (STEM HD 2700Cs, Hitachi), operated at an
205 acceleration voltage of 200 kV. Individual Ag-NPs, or their transformation products (Ag_2S)
206 were localized using a high-angle annular dark-field (HAADF) detector. Elemental analysis
207 of selected NPs was performed with an energy-dispersive X-ray (EDX) analysis system
208 (EDAX) attached to the microscope.

209 A few drops of the stock suspension were pipetted on a holey carbon TEM grid (Plano,
210 GmbH, Germany) and subsequently drawn through the grid by using a paper towel. After
211 particle deposition, the grid was washed with a drop of demineralized water. Two preparation
212 protocols were applied to deposit biofilm samples on TEM grids. The first protocol is very

simple and can be applied in any laboratory, however, it requires high particle concentrations due to the low amount of sample that is eventually retained on the TEM grid. The second protocol is more sophisticated and requires a dedicated infrastructure. However, suspension with much lower particle concentrations can successfully be prepared for STEM analyses, as the centrifugation procedure concentrates the particles from the suspension on the TEM grid.

In the first protocol, a few drops of the aqueous biofilm extracts obtained after the extraction with phosphate buffer were drawn through a TEM grid (Plano GmbH, Germany) with a paper towel. In the second protocol, the liquid samples (approximately 200 mL, duplicate samples from each microcosm were combined) were centrifuged (5 min at 700 x g) and the solid fraction was freeze dried and stored at -18°C. The samples were later thawed under a gentle argon flow, packed in moist absorbing clay and sent for further processing. The samples were ground to a fine powder with mortar and pestle. The powder was added to a 2.0 mL Eppendorf tube and filled with 1.6 mL of ultrahigh quality water (NANOpure, Diamond, Barnstead, Thermo Scientific). The dispersion was vortexed for 1 min and then split into 2 Eppendorf tubes. The two tubes were sonicated with a Hielscher UP200St Vial tweeter for 2 minutes (amplitude 75 %, cycle 50 %). Temperature was monitored during sonication in a separate tube filled with distilled water and the temperature did not rise above 45°C. The dispersions were diluted to reach final concentrations of ~0.3 mg sample/mL and 0.07 mg sample/mL. Two different concentrations were used to evaluate which one is better suited for the STEM analysis. These suspensions were centrifuged (1 h at 25,000 x g) on Formvar – Carbon coated TEM-grids (Quantifoil Micro Tools GmbH, Germany). The described treatment was necessary to evenly distribute the NPs on the TEM grid. Due to the grinding and sonication process, no conclusions can be drawn about the association between the (transformed) Ag-NPs and other colloids/particles in the original sample but the speciation of Ag-NPs should not change during sample preparation.

2.6 Data analysis

Statistical analyses were performed by using SPSS Statistics 22 software. Firstly, the data were examined for normal distribution using the Shapiro-Wilk's test. Because the normality criterion of all samples was not met, a non-parametric test (Mann-Whitney U) was performed. This test was done pairwise to determine whether the Ag mass in the effluent and in the different compartments of the microcosm differed significantly between the treatments. The level of significance was set at p=0.05.

3 Results

3.1 Characterization of Ag-NPs

The total Ag concentration of the stock Ag-NP suspension determined by ICP-MS was 97 ± 3 mg/L. Results from PCS measurements showed a number-weighted average particle diameter of ~10 nm (11.1 ± 0.2 nm). However, the intensity-weighted average particle diameter was close to 100 nm (90.9 ± 7.9 nm) indicating that also larger particles (most probably Ag-NP aggregates) were present in the stock suspension. The particle size distribution extracted from TEM images (~150 particles) revealed an average diameter of ~13 nm (Figure 1) confirming that intensity-weighted particle size distributions were biased by the presence of aggregates.

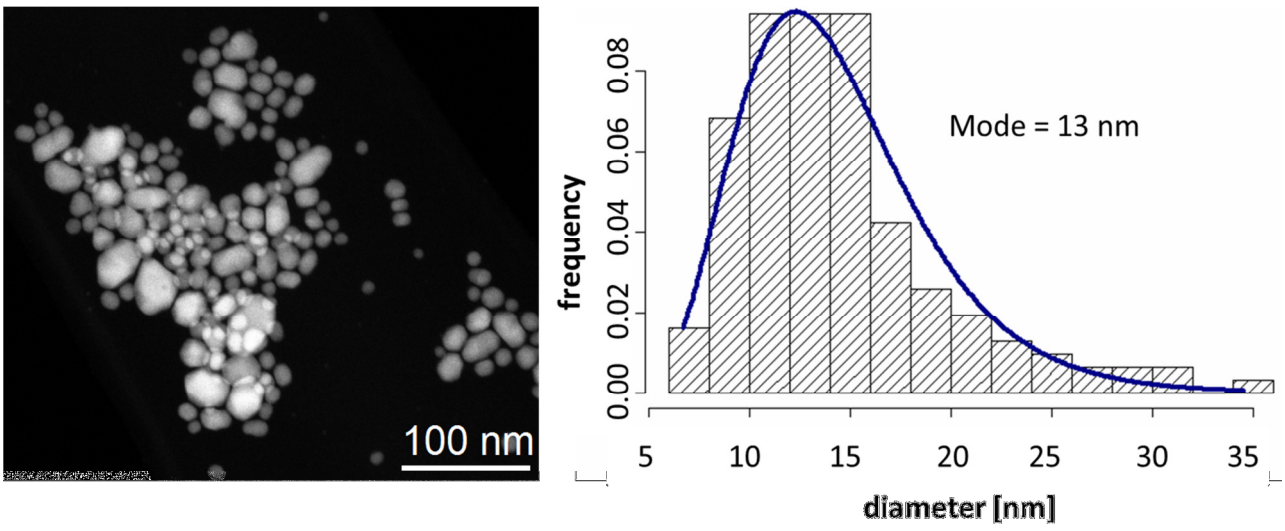

255 ***Figure 1 – Left: STEM image of the Ag-NP from the stock dispersion. Right: particle size distribution***
256 ***extracted from STEM images. The distribution was fitted to a log-normal distribution.***

257 **3.2 Dissolved oxygen (DO) and pH**

258 The influent had a pH of 8.0 whereas the pH of the effluents was slightly lower (7.4 – 7.7).
259 Due to the similarity of the effluent pH in all treatments, the pH is not considered to have
260 caused differences in the fate of Ag-NPs between the different treatments. In the aerated
261 treatments, the DO concentration was 3.2 ± 0.1 mg/L. Without aeration, the DO concentration
262 was 0 mg/L (detection limit reported by the manufacturer 0.1 mg/L).

263 **3.3 Total Ag concentration and removal of the Ag-NP in CWs**

264 After the initial acclimatization phase, 50 µg of Ag-NPs was spiked weekly during 18 weeks
265 resulting in a total nominal mass of 900 µg of Ag-NPs added to the microcosms (except for
266 the negative control). The Ag concentration in the influent water was measured in 15 out of
267 18 spiking events (due to technical difficulties) and resulted in an average mass of 52 ± 5 µg
268 of Ag applied per spiking event. For the mass balance calculations we assumed that an
269 average mass of 52 µg Ag was dosed in the microcosms in three spiking events where the
270 influent Ag concentration could not be measured. The total Ag concentration in the effluent
271 (measured at 15 events) and the effluent volume were used to calculate the mass of total Ag
272 leaving the microcosms. The total Ag mass released from the microcosms with the effluent
273 was lowest for the positive control and for the aerated microcosms, 90.5 ± 56.8 µg and 94.4 ±
274 17.8 µg, respectively (Table 2), and there was no significant difference between these
275 treatments ($p>0.05$). The highest total mass of Ag was measured in the effluent of the
276 microcosms with added OM, 190 ± 21.3 µg, which differed significantly from the other two
277 set-ups ($p<0.05$). For the three events where no Ag concentrations were available, we used the
278 average Ag concentrations in the effluent of the individual experiments to complete the mass
279 balance calculations. The Ag fractions retained in the wetland microcosms, calculated from

the difference between integrated influent and effluent Ag masses, were 0.8 and 0.9. The lowest removal (80 %) was obtained for the OM treatment and in the other two treatments (positive control and air) 90 % of the Ag was removed. The Ag concentrations measured in all samples from the negative controls were below the detection limit.

3.4 Distribution of Ag within the microcosms

The largest percentage of Ag that was recovered within the microcosms, was found in the biofilm extracts (Table 2). Independent of the treatment, approximately 95 % of the Ag recovered was associated with the substrate (sub-samples biofilm and gravel). The large standard deviation associated with the Ag mass in the gravel of the OM treatment is caused by one of the six sub-samples, where unusually high Ag concentrations were obtained (Table 2). A few % of Ag was lost to the biofilm that grew on the walls of the microcosms and less than 1 % was found in the plant roots. In the leaves and stems of the plants, the Ag concentrations remained below the detection limits.

293 ***Table 2 – The mass balance and distribution of total Ag within the microcosms. The total mass (µg Ag) is calculated for water and solid samples based on the measured***

294 ***concentration in the given medium and the volume or mass of the given medium.***

	Discharge and overall removal			[2]Distribution within the microcosm compartments										
Setup	**Influent**	**Effluent**	**[1]Removal efficiency**	**Biofilm**		**Gravel**		**Plant roots**		**Plant shoots**		**Microcosm walls**		**[3]Total recovery**
	µg Ag	µg Ag	%	µg Ag	%	µg Ag	%	µg Ag	%	µg Ag	%	µg Ag	%	%
Negative control	<LOD	<LOD	-	<LOD	-	<LOD	-	<LOD	-	<LOD	-	<LOD	-	-
Positive control	937±6	91±57	90	265±31	77	61±24	18	3.2±1.9	0.9	<LOD	-	17±6	4.9	49
OM	922±10	190±21	79	229±16	65	104±104	30	2.8±1.1	0.8	<LOD	-	16±1	4.5	61
Air	931±7	94±18	90	248±25	81	44±7	15	1.2±0.5	0.4	<LOD	-	11±9	3.7	44

295 **[1] Calculated from the difference between Ag masses measured in the influent and in the effluent**

296 **[2] Normalized by the sum of Ag mass recovered in the different microcosm compartments. The percentage represents the proportion of Ag mass recovered in a given**
297 **compartment to the sum of Ag mass recovered in all microcosm compartments.**

298 **[3] The percentage represents the proportion of Ag mass recovered in (effluent and all microcosm compartments) to the sum of Ag mass spiked (influent).**

299 **LOD: limit of detection**

300 **3.5 Correlation of TSS/TOC and total Ag content**

301 TSS and TOC were measured weekly between weeks 13 – 17 in the effluent samples. TSS
302 concentrations in the effluents of the positive control and the aerated treatments ranged from
303 3.7 to 178 mg/L, with the lowest values systematically measured in one of the three replicates
304 of the positive control. The high TSS concentration in the effluents of the OM setups (121 –
305 320 mg/L) demonstrates the effect of OM addition within the substrate. The solids in the
306 effluents of the positive control and the aerated treatments originate from biofilm, degrading
307 plant roots and potting soil that was still present between the roots upon planting. Similarly to
308 the TSS values, the TOC concentrations in the effluents of the positive control, aerated and
309 OM setups ranged from 4.7 to 97.9 mg/L, TOC being highest in the OM setups. A more
310 detailed overview of the TSS and TOC concentrations in the different treatments can be found
311 in the supplementary information section.

312 The total Ag concentration correlated well with the TSS concentration in the effluent
313 (R^2=0.81, Figure 2). Also Ag and TOC concentrations were positively correlated, but the
314 correlation was considerably less pronounced (R^2=0.59) compared to the correlation observed
315 between Ag and TSS. The Ag concentration in the filtrate from the TSS analysis was
316 analyzed twice during the experiment. The total Ag concentration in these filtrates was below
317 the detection limit in all samples (data not shown).

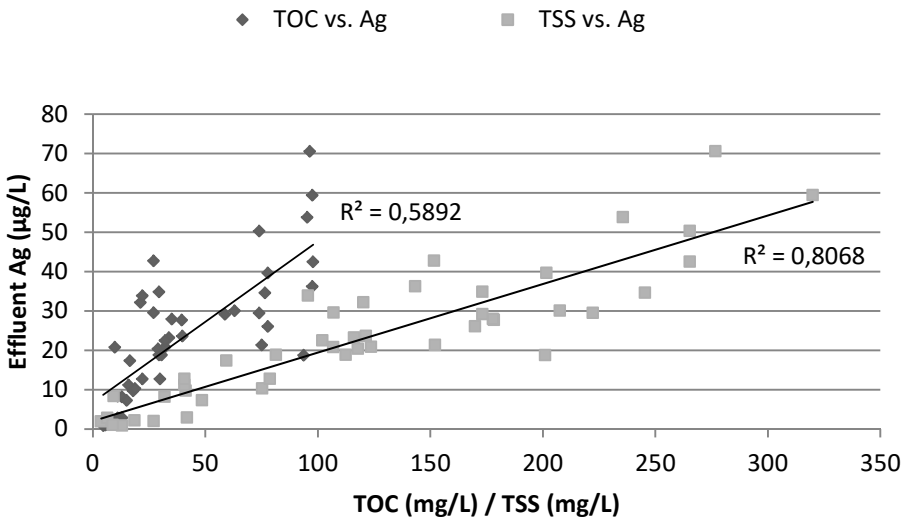

Figure 2 – Correlation between TSS or TOC and Ag concentration in microcosm effluents (n=45).

3.6 Morphology and elemental composition of Ag-NPs in the biofilm

The detected Ag-NPs were of comparable sizes as the pristine particles in the stock suspension (Figure 3). EDX analyses of individual particles revealed that Ag was always associated with sulfur (S), suggesting that Ag-NPs transformed into Ag_2S during the treatment. To a first approximation, the intensity ratio between S(Kα) and Ag(Lα) should reflect the atomic ratio of the transformed Ag-NPs. However, due to variable contributions of S from the background (organic matter) to the signal intensity, a quantitative evaluation of the signal intensities was not performed. Because of the presence of organic matter in the samples the recording of high resolution phase contrast images and phase identification based on lattice spacings was not possible. Thus, due to the small size of the particles and in combination with considerable amounts of S in the biofilms, the presence of minor amounts of metallic Ag (partially sulfidized Ag-NP) cannot be excluded.

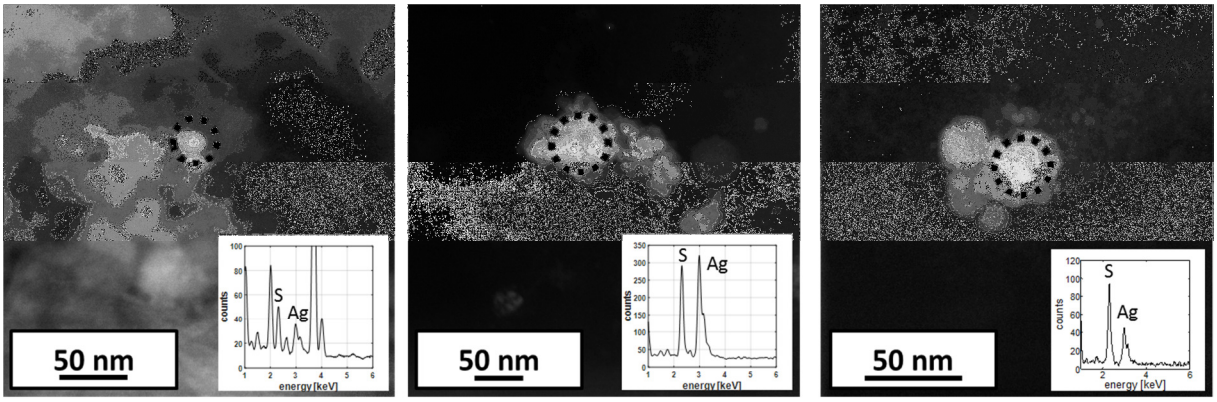

Figure 3 – STEM images (high angular annular dark field) of (transformed) Ag-NPs detected in the biofilm of the different microcosms (left: positive control; middle: OM; right: air). Insets show the EDX spectra of the particles marked with the dashed circle. The varying Ag – S ratios result from the variable background contribution of S which is present in the biofilm.

4 Discussion

Our results revealed an efficient retention of Ag-NPs in the CWs and indicated that most of the retained Ag-NPs were attached to/incorporated in the biofilm. However, in total only between 40 % and 60 % of the total Ag was recovered. The results from the Ag measurements in the influent were in agreement with the nominal mass applied in the microcosms. In the effluent samples, no residual materials were observed in the digested samples. We thus assume that results from the influent and effluent measurements were very robust. However, it is not clear whether the sequential extraction procedure quantitatively extracted the Ag from the gravel. Also, after the acid treatment of the emptied microcosms, remaining biofilm material was observed on the walls. In addition, the digestion protocol did not completely digest the plant material as residual particulate matter was observed in the digest. Thus, we assume that the poor mass balance closure for Ag resulted from the non-quantitative recovery of Ag from the different compartments within the microcosm, and thus did not affect the results of the Ag removal efficiencies calculated for the CWs from measured influent and effluent Ag concentrations.

352 The good correlation between the TSS and the Ag content in the effluent observed in all
353 experiments further suggests that Ag-NPs were dominantly attached to the particles/biomass
354 leaving the CWs which is in good agreement with earlier laboratory-, pilot- and full-scale
355 studies (e.g. Kaegi et al., 2011; Kim et al., 2010; Ma et al., 2014). In these studies it was
356 concluded that the Ag-NPs mainly accumulate in sludge and are therefore efficiently removed
357 from the water phase. This hypothesis is supported by the significantly higher Ag fraction that
358 passed the CWs in the OM treatment and the correspondingly lower fraction found in the
359 biofilm compared to the other treatments (Table 2). The addition of organic matter probably
360 provided additional surfaces for the attachment of Ag-NPs but also resulted in a higher
361 fraction of Ag that passed the CWs as more organic matter also left the CWs. However, the
362 Ag fractions extracted from the microcosm walls at the end of the experiments were
363 comparable for all three experiments (11 – 17 µg Ag) and may indicate that the addition of
364 OM did not substantially affect the biofilm, but mainly provided additional surfaces for Ag-
365 NP attachment. Furthermore, the total recovery of Ag was highest in the OM experiment,
366 which is in line with our hypothesis that the poor Ag mass closure is related to the incomplete
367 extraction/digestion of Ag from the compartments within the CWs. The higher Ag fraction
368 passing though the CWs in the OM experiment therefore resulted in reduced amounts of Ag
369 remaining in the CWs which in turn improved the mass closure of Ag.

370 In general, the high retention efficiencies of 80 % – 90 % of Ag-NPs in combination with the
371 fact that Ag-NPs are dominantly attached to organic matter are consistent with high annual
372 mean removal efficiencies (80 ± 15 %) of TSS reported from 17 CWs (Vymazal, 2009). The
373 results indicate that the retention of solids in the wetland becomes essential in limiting the
374 release of Ag (or particulate bound pollutants in general), which again is in line with the
375 absence of Ag in filtered effluents samples. The low concentrations detected in the filtrates
376 could be caused by adsorption of free Ag-NPs and Ag^+ on the paper filter. However, Van

Koetsem et al. (2016) has studied the recovery of these citrate-coated Ag-NPs and Ag^+ during filtration through the same paper filters as used in this study and they concluded that approximately 60 % and 95 % of Ag-NPs and Ag^+ were recovered in the filtrates, respectively. Hence, it is logical to assume that the low concentrations observed in the filtrates of this study indicate only negligible amounts of free Ag^+, and even Ag-NPs, in the samples.

Aeration did not result in an increased concentration of Ag in the water phase although aeration could have caused Ag^+ formation through oxidative dissolution of Ag-NPs (Liu et al., 2011). This can be well explained by the sulfidation of the Ag-NPs, which was also observed by STEM-EDX in samples from the aerated microcosms. Sulfidation results in dramatically reduced release of Ag^+ (Levard et al., 2011). As the DO in the aerated microcosms remained rather low (3.2 mg/L), it may well be possible that anoxic zones were present within the matrix or the biofilm where sulfate reducing bacteria may have developed.

In this study, we used citrate-coated Ag-NPs and another coating might stabilize Ag-NPs more efficiently. However, also polyvinylipyrrolidone (PVP) which sterically stabilizes the particles did not influence the removal efficiencies during activated sludge treatment (Kaegi et al., 2013) . Thus, we assume that our results are also applicable for Ag-NPs with other types of coatings.

5 Conclusions

Ag-NPs were very efficiently removed (80 - 90 %) from synthetic wastewater in microcosms simulating CWs. The largest fraction of Ag-NPs was attached to or incorporated in the biofilm developed on the gravel bed of the CWs. The fraction of Ag-NPs that passed the CWs, was bound to solids present in the effluent. Thus, an increasing retention of TSS in CWs would lead to a proportional decrease in Ag being discharged from the CWs. Results from STEM-EDX analyses suggested that Ag-NPs were dominantly sulfidized, even in the

aerated treatments. Anoxic/anaerobic zones within the biofilm most likely favored the growth of sulfate reducing bacteria resulting in the sulfidation of the Ag-NPs. Aeration did not affect the retention efficiency of total Ag in the microcosms and the distribution of total Ag in the aerated microcosms was similar to that of the positive control. The addition of OM provided additional surfaces for the attachment of Ag-NPs and resulted in a slightly reduced retention of Ag-NPs in the microcosms due to increased discharge of TSS with the effluent. Although this study describes laboratory-scale setups many conclusions and predictions on the fate of ENMs in full-scale CWs can be made. The biofilm is likely to function as the main sink for the Ag-NPs due to its high affinity for Ag-NPs. The biofilm thickness and the percentage of substrate covered by biofilm will increase with operation time and are thus higher in full-scale CWs than the studied microcosms, hence indicating larger biomass being able to accumulate Ag-NPs in full-scale CWs than in the microcosms studied. Also, plant roots, occupying a large volume in full-scale CWs, offer an important attachment site for biofilm and hence for Ag-NPs. As Ag-NPs are mainly accumulating in biofilm sudden high flow of influent, large fluctuations in aeration force or the presence of toxic compounds in the influent could induce the detachment of biofilm and hence, cause temporary release of (transformed) Ag-NPs from the CW. As the CW ages and more organic matter is accumulating within the CW bed, clogging could occur and lead to short-circuiting and possibly increased discharge of Ag-NPs. In general, the results obtained in this study implicate that the biofilm in CWs will act as a sink for Ag-NPs, similarly to activated sludge, and the release of (transformed) Ag-NPs is during normal operation primarily determined by the discharge of TSS.

Acknowledgements

We thank Ghent University for the PhD grant of H. Auvinen. We are thankful to the European Cooperation in Science and Technology (COST) for facilitating co-operation between

research institutes and would like to thank the members of the COST Action ES1205 Engineered Nanomaterials for fruitful discussions.

References

Anonymous. (n.d.). The Project of Emerging Nanotechnologies Consumer Product Inventory. Retrieved May 2, 2016, from http://www.nanotechproject.org/cpi

Auvinen, H., Sepúlveda, V. V., Rousseau, D. P. L., & Du Laing, G. (2016). Substrate- and plant-mediated removal of citrate-coated silver nanoparticles in constructed wetlands. *Environmental Science and Pollution Research*. http://doi.org/doi:10.1007/s11356-016-7459-6

Behra, R., Sigg, L., Clift, M. J. D., Herzog, F., Minghetti, M., Johnston, B., … Rothen-Rutishauser, B. (2013). Bioavailability of silver nanoparticles and ions: from a chemical and biochemical perspective. *Journal of the Royal Society, Interface / the Royal Society*, *10*(87), 20130396. http://doi.org/10.1098/rsif.2013.0396

Benn, T. M., & Westerhoff, P. (2008). Nanoparticle silver released into water from commercially available sock fabrics. *Environmental Science and Technology*, *42*(11), 4133–4139. http://doi.org/10.1021/es7032718

Blaser, S. A., Scheringer, M., MacLeod, M., & Hungerbühler, K. (2008). Estimation of cumulative aquatic exposure and risk due to silver: Contribution of nano-functionalized plastics and textiles. *Science of the Total Environment*, *390*(2–3), 396–409. http://doi.org/10.1016/j.scitotenv.2007.10.010

Button, M., Auvinen, H., Koetsem, F. Van, Hosseinkhani, B., Rousseau, D., Weber, K. P., & Du, G. (2016). Susceptibility of constructed wetland microbial communities to silver nanoparticles : A microcosm study. *Ecological Engineering*, *97*, 476–485. http://doi.org/10.1016/j.ecoleng.2016.10.033

Colvin, V. L. (2004). The potential environmental impact of engineered nanomaterials. *Nature Biotechnology*, *22*(6), 760–760. http://doi.org/10.1038/nbt0604-760c

Doiron, K., Pelletier, E., & Lemarchand, K. (2012). Impact of polymer-coated silver nanoparticles on marine microbial communities: A microcosm study. *Aquatic Toxicology*, *124–125*, 22–27. http://doi.org/10.1016/j.aquatox.2012.07.004

Du Laing, G., Tack, F. M. G., & Verloo, M. G. (2003). Performance of selected destruction methods for the determination of heavy metals in reed plants (Phragmites australis). *Analytica Chimica Acta*, *497*(1–2), 191–198. http://doi.org/10.1016/j.aca.2003.08.044

Fan, J., Zhang, B., Zhang, J., Ngo, H. H., Guo, W., Liu, F., … Wu, H. (2013). Intermittent aeration strategy to enhance organics and nitrogen removal in subsurface flow constructed wetlands. *Bioresource Technology*, *141*(August 2015), 117–122. http://doi.org/10.1016/j.biortech.2013.03.077

Kadlec, R. H., & Wallace, S. D. (2009). *Treatment Wetlands* (2nd ed.). Boca Raton: CRC Press. http://doi.org/10.1201/9781420012514

Kaegi, R., Voegelin, A., Ort, C., Sinnet, B., Thalmann, B., Krismer, J., … Mueller, E. (2013). Fate and transformation of silver nanoparticles in urban wastewater systems. *Water*

Research, *47*(12), 3866–3877. http://doi.org/10.1016/j.watres.2012.11.060

Kaegi, R., Voegelin, A., Sinnet, B., Zuleeg, S., Hagendorfer, H., Burkhardt, M., & Siegrist, H. (2011). Behavior of metallic silver nanoparticles in a pilot wastewater treatment plant. *Environmental Science and Technology*, *45*(9), 3902–3908. http://doi.org/10.1021/es1041892

Kim, B., Park, C. S., Murayama, M., & Hochella, M. F. (2010). Discovery and characterization of silver sulfide nanoparticles in final sewage sludge products. *Environmental Science and Technology*, *44*(19), 7509–7514. http://doi.org/10.1021/es101565j

Levard, C., Reinsch, B. C., Michel, F. M., Oumahi, C., Lowry, G. V., & Brown, G. E. (2011). Sulfidation processes of PVP-coated silver nanoparticles in aqueous solution: Impact on dissolution rate. *Environmental Science and Technology*, *45*(12), 5260–5266. http://doi.org/10.1021/es2007758

Li, L., Hartmann, G., & Schuster, M. (2013). Quantification of Nanoscale Silver Particles Removal and Release from Municipal Wastewater Treatment Plants in Germany. *Environmental Science & Technology*, *47*, 7317–7323.

Liu, J., Pennell, K. G., & Hurt, R. H. (2011). Kinetics and mechanisms of nanosilver oxysulfidation. *Environmental Science and Technology*, *45*(17), 7345–7353. http://doi.org/10.1021/es201539s

Lombi, E., Donner, E., Taheri, S., Tavakkoli, E., Jämting, A. K., McClure, S., … Vasilev, K. (2013). Transformation of four silver/silver chloride nanoparticles during anaerobic treatment of wastewater and post-processing of sewage sludge. *Environmental Pollution*, *176*, 193–197. http://doi.org/10.1016/j.envpol.2013.01.029

Lowry, G. V., Espinasse, B. P., Badireddy, A. R., Richardson, C. J., Reinsch, B. C., Bryant, L. D., … Wiesner, M. R. (2012). Long-term transformation and fate of manufactured Ag nanoparticles in a simulated large scale freshwater emergent wetland. *Environmental Science and Technology*, *46*(13), 7027–7036. http://doi.org/10.1021/es204608d

Lowry, G. V., Gregory, K. B., Apte, S. C., & Lead, J. R. (2012). Transformations of Nanomaterials in the Environment. *Environmental Science & Technology*, *46*(13), 6893–6899. http://doi.org/10.1021/es300839e

Ma, R., Levard, C., Judy, J. D., Unrine, J. M., Durenkamp, M., Martin, B., … Lowry, G. V. (2014). Fate of Zinc Oxide and Silver Nanoparticles in a Pilot Wastewater Treatment Plant and in Processed Biosolids. *Environmental Science & Technology*, *48*(1), 104–112. http://doi.org/10.1021/es403646x

Mitrano, D. M., Rimmele, E., Wichser, A., Erni, R., Height, M., & Nowack, B. (2014). Presence of nanoparticles in wash water from conventional silver and nano-silver textiles. *ACS Nano*, *8*(7), 7208–7219. http://doi.org/10.1021/nn502228w

Nivala, J., Hoos, M. B., Cross, C., Wallace, S., & Parkin, G. (2007). Treatment of landfill leachate using an aerated, horizontal subsurface-flow constructed wetland. *Science of the Total Environment*, *380*(1–3), 19–27. http://doi.org/10.1016/j.scitotenv.2006.12.030

OECD. (2001). *OECD guidelines for the testing of chemicals - 303A Activated sludge units*. OECD Publishing. http://doi.org/9789264070424

Peralta-Videa, J. R., Zhao, L., Lopez-Moreno, M. L., de la Rosa, G., Hong, J., & Gardea-Torresdey, J. L. (2011). Nanomaterials and the environment: A review for the biennium

2008–2010. *Journal of Hazardous Materials*, *186*(1), 1–15. http://doi.org/10.1016/j.jhazmat.2010.11.020

Ratte, H. T. (1999). Bioaccumulation and toxicity of silver compounds: A review. *Environmental Toxicology and Chemistry*, *18*(1), 89–108. http://doi.org/10.1002/etc.5620180112

Reinsch, B. C., Levard, C., Li, Z., Ma, R., Wise, a., Gregory, K. B., … Lowry, G. V. (2012). Sulfidation of silver nanoparticles decreases Escherichia coli growth inhibition. *Environmental Science and Technology*, *46*(13), 6992–7000. http://doi.org/10.1021/es203732x

Van Koetsem, F., Geremew, T. T., Wallaert, E., Verbeken, K., Van der Meeren, P., & Du Laing, G. (2015). Fate of engineered nanomaterials in surface water: Factors affecting interactions of Ag and CeO2 nanoparticles with (re)suspended sediments. *Ecological Engineering*, *80*, 140–150. http://doi.org/10.1016/j.ecoleng.2014.07.024

Van Koetsem, F., Verstraete, S., Wallaert, E., Verbeken, K., Van Der Meeren, P., Rinklebe, J., & Du Laing, G. (2016). Use of filtration techniques to study environmental fate of engineered metallic nanoparticles: Factors affecting filter performance. *Journal of Hazardous Materials*. http://doi.org/10.1016/j.jhazmat.2016.05.098

Vymazal, J. (2009). The use constructed wetlands with horizontal sub-surface flow for various types of wastewater. *Ecological Engineering*, *35*(1), 1–17. http://doi.org/10.1016/j.ecoleng.2008.08.016

Wagner, T. (2016). ij-particlesizer: ParticleSizer 1.0.3 Zenodo. http://doi.org/10.5281/zenodo.56457

Zhang, L. yu, Zhang, L., Liu, Y. ding, Shen, Y. wu, Liu, H., & Xiong, Y. (2010). Effect of limited artificial aeration on constructed wetland treatment of domestic wastewater. *Desalination*, *250*(3), 915–920. http://doi.org/10.1016/j.desal.2008.04.062